



SEISMIC EVALUATION OF VULNERABLE HIGHWAY BRIDGES WITH WALL PIERS ON EMERGENCY ROUTES IN SOUTHERN ILLINOIS

John L. BIGNELL¹, James M. LAFAVE², Joseph P. WILKEY³, and Neil M. HAWKINS⁴

SUMMARY

To assess the seismic vulnerability of priority emergency routes in southern Illinois, the Illinois Department of Transportation (IDOT) has initiated several research projects whose aim has been to determine the vulnerability of typical bridge structures found on those routes. From a 10% random sample it has been determined that the two most common types of bridge structures found on those routes are multi-column pier supported (58%) and wall pier supported (28%). An earlier project completed the construction of analytical fragility curves for the multi-column structures under expected New Madrid Seismic Zone (NMSZ) ground motions. This paper presents preliminary findings from the current research project, which is producing similar curves for the wall pier structures. Characteristics of wall pier supported bridges on priority emergency routes in southern Illinois are presented, and an overview is given of the procedure used to construct the fragility curves produced in this study. Fragility curves and analytical pushover results for an individual two-span non-skew wall pier supported bridge, typical of those found on southern Illinois priority emergency routes, are presented. Finally, general implications of the conclusions from the previous and current studies on the state of the priority emergency route network in southern Illinois are given.

INTRODUCTION

For many years now, the Midwestern U.S. has been recognized as the location of a possibly devastating seismic event. This realization is due, in no small part, to the events of late 1811 and early 1812, in which a series of large earthquakes (at least one with an estimated moment magnitude of 7.9) occurred along the New Madrid Fault. These earthquakes had an unusually large area of damage, up to three times that of the

¹ Graduate Research Assistant; University of Illinois at Urbana-Champaign, Department of Civil and Environmental Engineering; Urbana, Illinois, 61801, U.S.A.; bignell@uiuc.edu

² Assistant Professor; University of Illinois at Urbana-Champaign, Department of Civil and Environmental Engineering; Urbana, Illinois, 61801, U.S.A.; jlafave@uiuc.edu; (phone) 1-217-333-8064; (fax) 1-217-265-8039

³ Undergraduate Research Assistant; University of Illinois at Urbana-Champaign, Department of Civil and Environmental Engineering; Urbana, Illinois, 61801, U.S.A.; jwilkey@uiuc.edu

⁴ Professor Emeritus; University of Illinois at Urbana-Champaign, Department of Civil and Environmental Engineering; Urbana, Illinois, 61801, U.S.A.; nmhawkin@uiuc.edu

1964 Alaska Earthquake (the largest earthquake in the United States, with moment magnitude 9.2) and up to ten times that of the famous 1906 San Francisco Earthquake (which had a similar moment magnitude of 7.7) [1]. The 1811-1812 earthquakes were felt by people over an area of 1 million square miles. Large regions of land experienced uplifts of over 9 feet, while others experienced significant liquefaction and subsidence [2]. Due to the sparsity of population and built environment, large-scale loss of life and property was avoided. However, a similar event today would likely be devastating. Although it has been nearly 200 years since a major earthquake has occurred in the region, the New Madrid Seismic Zone (NMSZ) continues to be seismically active and to pose a serious threat.

The southern half of the state of Illinois is within the region of impact of this seismic zone. Therefore, as part of an earthquake preparedness plan, the Illinois Department of Transportation (IDOT) has designated

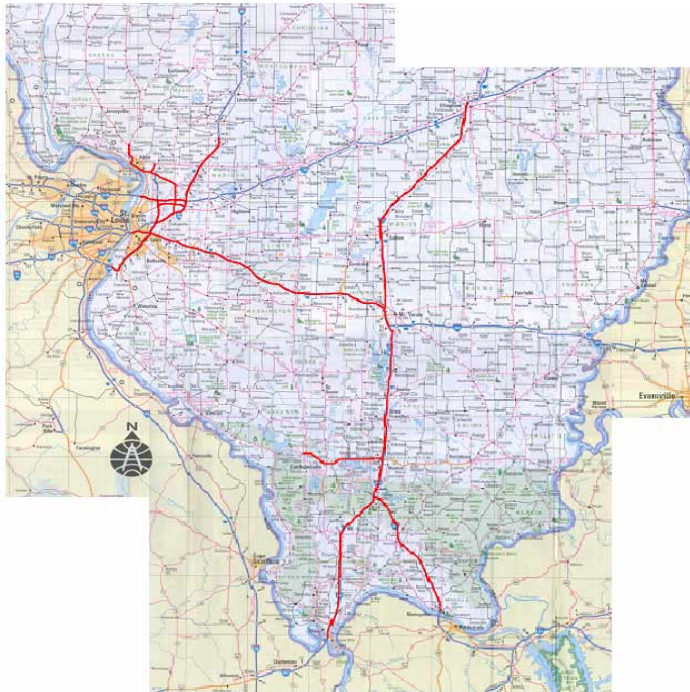


Figure 1 Southern Illinois Priority Emergency Routes

several transportation routes in the seismically susceptible southern portion of the state as emergency priority routes (Figure 1) [3]. In the event of an earthquake, these routes are to remain functional so that emergency personnel and supplies can effectively and efficiently reach areas in need.

As a first step in the assessment of the vulnerability of these routes to seismic events, several research projects were initiated. As part of one of those projects in the Mid-America Earthquake (MAE) Center, conducted by Qun Zhong and Neil Hawkins and completed in 2001, an inventory of all bridges found on priority emergency routes in southern Illinois was constructed [4]. It was determined that four basic types of bridge structures exist. They were reported as multi-column pier supported, wall pier supported, culvert, and single span. Figure 2 shows a typical multi-

column pier, while Figure 3 shows several typical wall piers. Since it had been determined that multi-column piers were the most prevalent bridge type, Zhong's research focused on determining the vulnerability of that type of bridge to expected NMSZ ground motions. The current project is aimed at assessing the seismic vulnerability of wall pier supported bridges, the second most prevalent bridge type found on Illinois priority emergency routes.

PREVIOUS MULTI-COLUMN PIER SUPPORTED BRIDGE PROJECT

To quantify the expected seismic performance of multi-column pier supported bridges in southern Illinois, Zhong carried out the following steps [4]:

1. Characteristics of southern Illinois multi-column pier supported bridges were determined by collecting detailed information from a 10% random sample of bridges on southern Illinois priority emergency routes.
2. Multi-column bridge pier structural component vulnerabilities were assessed, using nonlinear static pushover analyses.

3. Probabilities of reaching or exceeding various structural damage states for expected NMSZ ground shaking were determined using an analytical fragility analysis.
4. Multi-column pier damage levels were correlated with expected loss of bridge functionality.
5. The above analyses were repeated for bridges employing several column wrapping retrofit strategies, using the comparative results to quantify the effectiveness of each.

Zhong found that typical southern Illinois multi-column pier supported bridges were susceptible to NMSZ earthquakes with a 2% probability of exceedance (PE) in 50 years, whereas events with a 10% PE in 50 years would cause relatively minor damage. The damage expected in the larger earthquakes was due to various structural deficiencies. For a 2% PE in 50 years event, approximately 61% of the piers would experience column lap-splice failures, 12% would experience column shear failures, and 8% would experience cap beam shear failures. For a similar level of shaking, 56% of the multi-column piers would experience bearing shear failures, and 10% would experience rocker bearing overturning failures. Piles were also vulnerable to damage - 35% of the piers would experience pile tension failures, 30% would experience excessive rotation of plastic hinges in the piles, 12% would experience pile shear failures, 8% would experience pile overload failures, and 38% would experience local soil yielding around the piles. Finally, 19% of the piers would experience excessive drift.

Based on these analytical results, it was reported that in a 2% PE in 50 years event, a typical multi-column pier supported bridge would have a 61% probability of experiencing major damage, a 70% probability of experiencing at least moderate damage, and an 82% probability of experiencing at least minor damage.

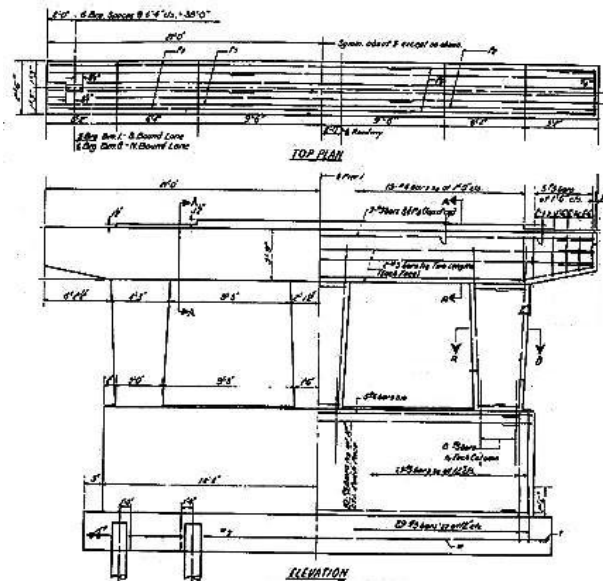


Figure 2 Typical Multi-Column Pier

SOUTHERN ILLINOIS HIGHWAY BRIDGE CHARACTERISTICS

A project currently underway has reported the total number of bridges on southern Illinois priority emergency routes as 595. For the multi-column pier supported bridge project, Zhong constructed a 10% random sample of bridges on priority emergency routes in southern Illinois; a total of 51 bridges comprised that sample.¹ Multi-column pier supported, wall pier supported, single span, culvert, and “other” made up 58%, 28%, 6%, 6%, and 2% of the bridges in the sample, respectively. Structural drawings were retrieved from IDOT for the wall pier supported bridges in the sample so that detailed structural characteristics could be determined [5].

Wall Pier Supported Bridges - Typical Characteristics

From the wall pier supported bridge sample, it was determined that three general categories of wall piers exist, namely *hammerhead*, *regular*, and *flexible* (Figure 3). Of the total number of wall pier supported

¹ Zhong originally reported the total number of bridges on southern Illinois priority routes as 519, thus 51 bridges was approximately 10% of that total.

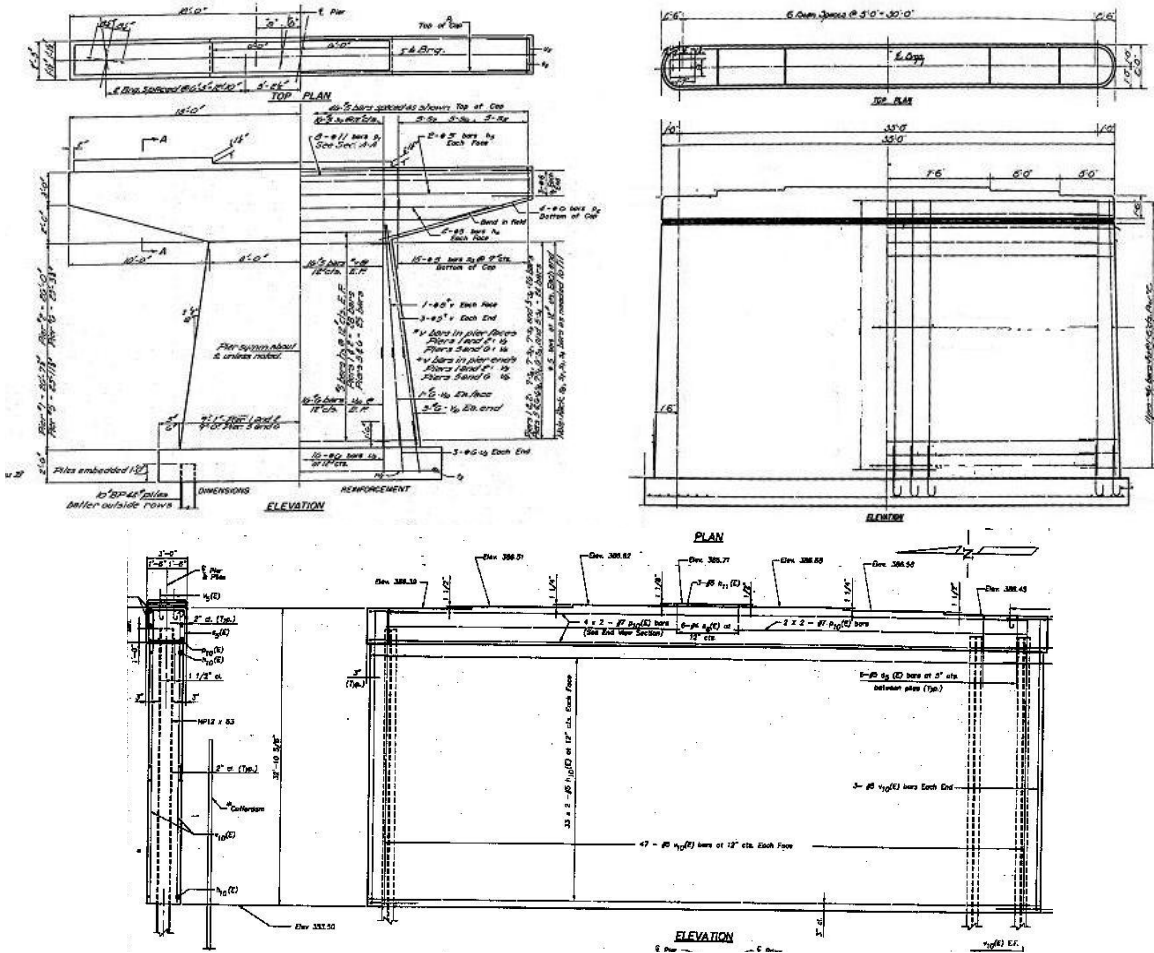


Figure 3 Hammerhead Wall Pier (Top Left), Regular Wall Pier (Top Right), and Flexible Wall Pier (Bottom).

bridges, hammerhead wall pier bridges made up 46%, regular wall pier bridges made up 46%, and flexible wall pier bridges made up 8%.

Nearly all of the wall pier bridges in the sample were constructed before 1975 (82%). The vast majority of the bridges had one to three piers (95%). Half of the bridges spanned waterways, and those bridges typically had two piers. The other half of the bridges spanned roads and typically had one or three piers. Most bridges in the sample had a skew angle less than or equal to 20 degrees (82%), with a majority having skew angles of 10 degrees or less (64%). The maximum skew angle encountered was 43 degrees.

Most wall pier bridges in the sample had pile foundations (86%); the remaining bridges surveyed utilized a conventional shallow mat foundation. Of the piers that utilized piles, steel and timber piles were the most prevalent types (48% and 42% of the pile-supported piers, respectively). The number of foundation piles employed was modest, with most of the pile-supported piers having less than 25 (>70% of the piers). The average pile length was 36 feet. The majority of the piers had piles with embedment depths into the pile cap of 12 inches (63% of the piers).

Nearly all of the wall pier bridges in the sample had lap splices in the pier wall vertical steel, between the footing or pile cap and the base of the wall (91% of the wall piers). Typical lap splice l/d_b ratios ranged from 31 to 50 (72%). The wall pier dimensions varied significantly. The average height was 222 inches

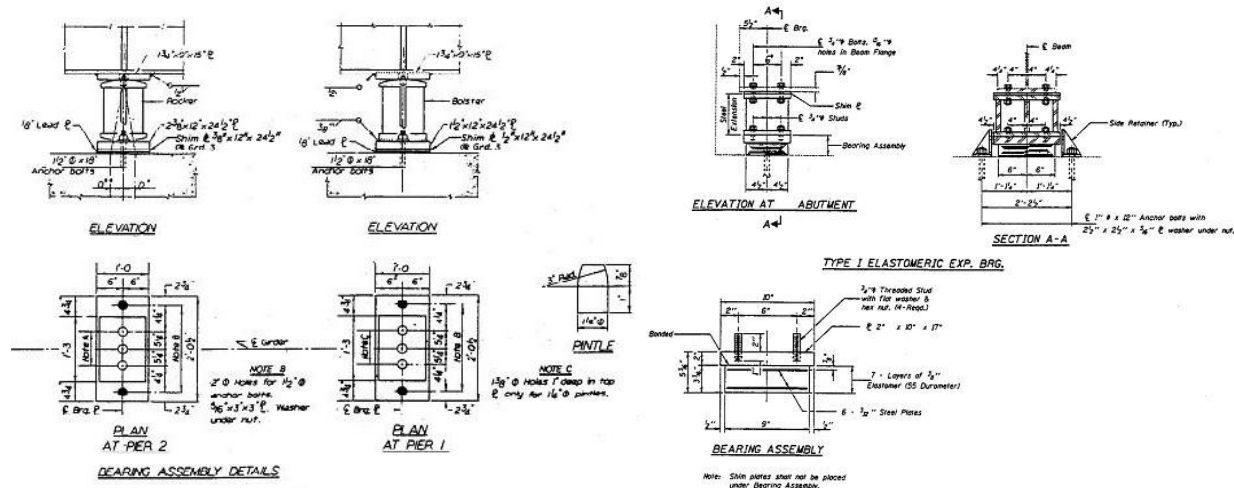


Figure 4 High Type Steel Rocker and Bolster Bearings (Left) and Illinois Type I Elastomeric Bearing (Right)

(about 18.5 feet), the average thickness was 33.5 inches (approximately 3 feet), and the length ranged from 168 inches (14 feet) to 678 inches (56.5 feet). The wall piers had extremely light reinforcement by today's standards. The average vertical steel ratio was 0.24% and the average horizontal steel ratio was 0.15%. No transverse reinforcing steel (through the thickness of the wall) was encountered.

High steel rocker and high steel bolster type bearings (Figure 4) were by far the most prevalent bearing types encountered in use between the superstructure and the wall piers (92% of the piers). Elastomeric bearings (Figure 4) were more frequently used at the abutments (33% of the abutments); however, high steel rocker bearings still made up the majority of the abutment bearings used (62% of the abutments).

The vast majority of wall pier bridges in the sample had two expansion joints (86% of the bridges). The expansion joints were typically located between the abutments and the superstructure, with the majority of the expansion joints having a gap of 1.5 inches.

Steel piles were the most prevalent abutment pile type (59% of the abutments) used in wall pier bridges. Typically from 6 to 15 piles were employed in the abutments (64% of the abutments). The average pile length was about 48 feet. The predominant reinforcing steel yield stress was 40 ksi (77% of the bridges). All bridges in the sample had specified concrete compressive strength (f_c') values in the range from 3000 to 3500 psi.

IDOT Bridge 067-0021 Characteristics

IDOT bridge 067-0021 is located in Monroe County, near East St. Louis. The structure is a non-skew two-span regular wall pier supported bridge. The central pier is supported on 21 concrete filled steel pipe piles, with an average length of 51 feet. The pile embedment depth into the pile cap is 12 inches. The wall pier is 22 feet 9 inches tall, 3 feet 4 inches thick, and 29 feet 2¾ inches long with a vertical steel-reinforcing ratio of 0.30% and a horizontal steel reinforcing ratio of 0.09%. A lap splice exists between the footing and the pile cap, with an l/d_b ratio of 41. Low type steel bearings (similar to the high type steel bearing shown earlier except the vertical dimension of the bearing is approximately ¼ that of the high type steel bearing) are used between the pier and the superstructure, and Illinois Type I elastomeric bearings are used between the superstructure and abutments. The superstructure comprises two expansion joints, one at each abutment. The expansion joint gap size is 2¾ inches. The abutments employ 18 piles each. Finally, f_c' is 3500 psi and the steel reinforcement yield stress is 60 ksi.

The local soil conditions at the IDOT bridge 067-0021 site are typified by alluvial sand deposits of between 5 and 12 feet thick, with relatively low unadjusted standard penetration test (SPT) blow count values of between 4 and 12. These layers are underlain by a 19 foot thick alluvial sand and gravel deposit with unadjusted SPT blow count values of between 27 and more than 100. The ground water table at the time the borings were taken was measured at approximately 8 feet below the bottom of the pile cap. While the water table can be expected to fluctuate significantly, all of the liquefiable soil layers exist below the measured water table level and at least a portion of those soils would be expected to be fully saturated at all times.

ANALYTICAL WALL PIER BRIDGE MODEL

The general purpose finite element analysis program ABAQUS [6] was used for the analyses of IDOT bridge 067-0021. A fully three-dimensional nonlinear model was constructed, incorporating all of the following major components: approach embankments/abutments, expansion joints, bearings, superstructure, wall piers, footings, and pile foundations. An extensive literature review was conducted to determine appropriate models and modeling techniques for representing each of these components analytically [7]. The following briefly describes the models used.

The ATC-32 [8] abutment model was used for representing the behavior of the abutments [9]. In the ATC-32 model, the transverse and longitudinal stiffness and capacity of an abutment is represented by several nonlinear equivalent springs. The stiffnesses and capacities of these springs are determined from wing wall and back wall dimensions, the number of piles employed in the abutment, and an average soil stiffness and pressure capacity. The dynamic contribution of the embankment soil mass is not considered.

Simple ABAQUS [6] nonlinear spring and truss elements were used to model the expansion joint behavior. The models were created in conjunction with the recommendations made in ATC-32 [8] for modeling expansion joints.

The low type steel bearings were modeled using the methodology outlined by Mander et al. [10]. In this model, bearing behavior is represented using simple nonlinear truss and link elements. Theoretical bearing strengths and stiffnesses are obtained based on simple strength of materials and solid mechanics considerations. The elastomeric bearings were modeled using the methodologies outlined by Wissawapaisal [11] and by Ash et al. [12], where bearing behavior was modeled using simple nonlinear truss elements with stiffnesses determined from simple mechanics of materials considerations.

Based on the recommendations of ATC-32 [8], it is considered unlikely that the superstructure will behave in a nonlinear fashion under the expected seismic loadings, so it will therefore probably only act as a linear elastic membrane through which seismic loads are transferred to the various supporting portions of the structure. For this reason, linear elastic shell elements, in conjunction with linear elastic beam elements, were used to model the superstructure [6].

The wall pier was modeled using a combination of linear and nonlinear shell elements with embedded nonlinear reinforcement. A nonlinear concrete constitutive model was used in regions of the wall where large concrete strains were expected. The pile cap model used linear elastic shell elements [6].

For the piles and soil-pile interaction, the widely used Beam on Nonlinear Winkler Foundation (BNWF) model was employed. The BNWF method models the piles using linear or nonlinear beam-column elements (linear for bridge 067-0021 presented in this paper), while the surrounding soil is modeled using nonlinear springs and dashpots. The BNWF model represents the current standard-of-practice in modeling pile-supported foundations [8, 13-15]. Kornkasem [15] found that far-field soil effects had only a minor

effect on bridge response for typical earthquake frequency contents and non-stiff soils; therefore the far field soil model was not included. Recommendations found in ATC-32 [8] state that pile group effects are small (on the order of 20%) for modest pile groups that have center-to-center pile spacings of three pile diameters, and also for non-stiff soils; furthermore, during cyclic loading these group effects are reduced. Therefore, modifications to the p-y, t-z, and q-z curves to account for group effects were not included in the model.

Concrete was modeled in ABAQUS [6] using either a linear elastic model with a reduced modulus to account for cracking, or in areas where large concrete strains were expected, the smeared cracking concrete model was employed. The smeared cracking model treats the tensile and compressive responses of concrete separately. In tension, the concrete is assumed to act linearly until a specified stress limit is reached, at which point the model assumes the material has cracked. The post-cracking response, defined by the user, includes “tension stiffening” to capture the average interaction of steel and concrete across cracks. In compression, the material acts in a nonlinear manner; however, degradation of the unloading elastic stiffness as the compressive strain magnitude increases is not accounted for in the model.

Steel was modeled using the ABAQUS [6] classical metal plasticity model. In this model, the steel behavior is assumed to be linear elastic up to the yield stress defined by either the von Mises or Hill yield surfaces, at which point the material flows plastically. Perfect plasticity, isotropic hardening, or linear kinematic hardening can be defined for the plastic portion of the material behavior. Reinforcing steel utilized the classical metal plasticity model with isotropic hardening. Several of the other bridge component models (e.g., the bearing and/or soil models) utilized the classical metal plasticity model with either kinematic hardening or perfectly plastic behavior.

PUSHOVER ANALYSES FOR IDOT BRIDGE 067-0021

Both longitudinal and transverse pushover analyses have been conducted for IDOT bridge 067-0021. To perform these pushover analyses, a gravity load representing the dead weight of the structure (no live load) was first applied, followed by the application to the superstructure and wall pier of a horizontal acceleration. The applications of these loads were carried out in a static analysis step [6]. The horizontal accelerations are similar to an applied gravitational force except they act horizontally on the structure. For each pushover analysis, the applied acceleration is ramped up linearly until the structure can no longer carry additional load.

Figure 5 (left plot) shows the results of the longitudinal direction pushover analysis. The forces transmitted to the pier, to abutment 1, and to abutment 2 are each plotted versus the displacement of the

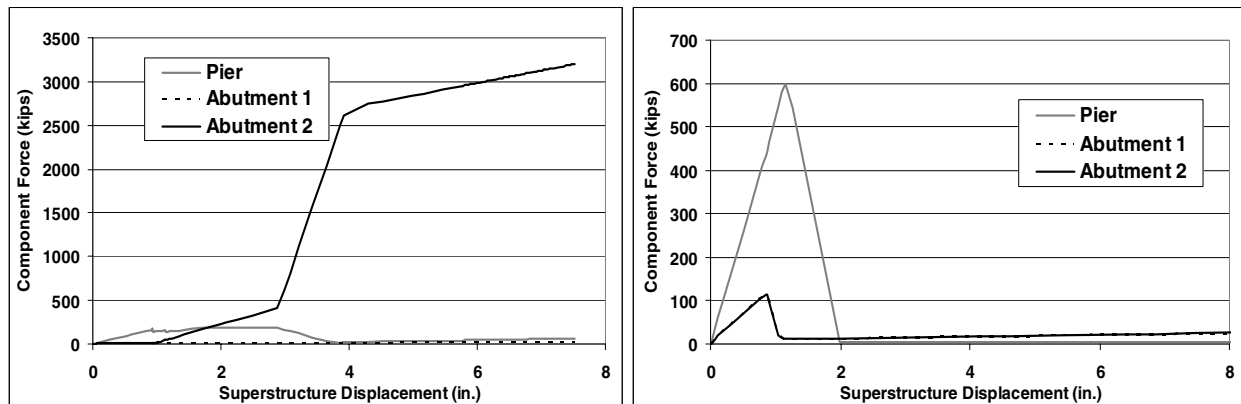


Figure 5 Longitudinal (Left) and Transverse (Right) Pushover Results.

superstructure. It is clear from the graph that abutment 2 carried the vast majority of the applied load once the expansion joint gap (2.75 inches) at that abutment had closed. The sequence of events leading to total failure were as follows: axial-moment loading pile failure near the pile cap/pile interface followed by expansion joint gap closure at abutment 2, pile cap negative moment bending failure at the wall face, abutment 2 exceedance of capacity failure, and finally wall pier failure based on ductility.

Figure 5 (right plot) shows the results of the transverse direction pushover analysis. The forces transmitted to the pier, to abutment 1, and to abutment 2 are each plotted versus the displacement of the superstructure. During loading, the abutments and the wall pier/wall pier foundation system exhibited very little nonlinearity. The sequence of events leading to total failure were as follows: axial-moment loading pile failure near the pile cap/pile interface followed by failure of the elastomeric bearing retainer brackets at the abutments, then shear failure of the pier low type fixed steel bearings, and finally loss of seat at the pier and abutments.

ANALYTICAL FRAGILITY CURVE CONSTRUCTION

A methodology for the construction of analytical fragility curves (similar to that outlined by Choi et al. [16]) was used for the construction of the fragility curves presented here for IDOT bridge 067-0021. The particular steps outlined below were carried out:

1. Construct representative numerical model.
2. Locate appropriate ground motions representative of NMSZ earthquakes.
3. Calculate soil layer ground motions using appropriate site response software.
4. Perform nonlinear dynamic time history analyses for each model-earthquake pair.
5. Use results from all model-earthquake pairs to determine relationships between component demand and earthquake magnitude.
6. Use the derived relationship in step 5 to construct component fragility curves.
7. Use first order reliability theory to construct structure fragility curves from component fragility curves.

Information pertaining to step 1 has been presented above. Bedrock ground motions for step 2 were acquired for the NMSZ cities of St. Louis, Carbondale, and Memphis, from another MAE Center project [17]. To accomplish step 3, the equivalent linear site response software SHAKE2000 [18] was used to calculate soil layer motions near the ground surface from these bedrock motions. The bedrock motions were used as input at the base of the soil columns specified in the set of boring logs obtained for IDOT bridge 067-0021. The depth to the base of the soil column was approximately 50 feet. Once the motions had been determined for each soil layer, a random angle between 0 and 90 degrees was assigned to each earthquake. The assigned angle was then used to calculate the longitudinal and transverse component of the ground motion at each soil layer for input into the model. Step 4 was carried out by running nonlinear implicit dynamic analyses in the general-purpose finite element program ABAQUS (Version 6.4) for 14 model-earthquake pairs.

Several component limit states were used for the completion of step 5. Component limit states were defined for the wall pier, pile cap, piles, bearings, and abutments. Wall pier limit states were based on strength and ductility limits derived from several in-plane and out-of-plane experiments carried out by Haroun et al. [19] and Abo-Shadi et al. [20], the nominal shear and moment strength equations outlined in ACI 318-02 [21], and reinforcing bar anchorage equations outline by Alsiwat and Saatcioglu [22]. Pile cap shear and bending limit states were based on nominal strength equations outlined in ACI 318-02 [21]. Pile limit states (axial force and moment loading interaction failure, shear failure, and pile anchorage failure) were based on equations outlined by Viest et al. [23] for concrete filled steel pipe piles subjected

Damage State	Definition
None	No damage
Slight/Minor	Minor cracking and spalling to the abutment, cracks in shear keys at abutments, minor spalling and cracks at hinges, minor spalling at the column (damage requires no more than cosmetic repair), or minor cracking to deck.
Moderate	Any column experiencing moderate cracks (shear cracks), cracking and spalling (column structurally still sound), moderate movement of the abutment (<2 inches), extensive cracking and spalling of shear keys, any connection having cracked shear keys or bent bolts, keeper plate failure without unseating, rocker bearing failure, or moderate settlement of the approach.
Extensive	Any column degrading without collapse - shear failure - (column structurally unsafe), significant residual movement at connections, or major settlement of approach, vertical offset of the abutment, differential settlement at connections, shear key failure at abutments.
Complete	Any column collapsing and connection losing all bearing support, which may lead to imminent deck collapse, tilting of substructure due to foundation failure.

Table 1 Damage States According to HAZUS99

to axial loading and moments, shear equations outlined by the same authors, and capacity considerations of the anchorage details, respectively. Bearing limit states (anchor bolt shear failure, anchor bolt fracture due to the combined actions of prying and shear, anchor bolt pullout, pintle shear failure, toppling, and loss of seat) were based on the equations outlined by Mander et al. [10], equations outlined in the AISC LRFD specification [24], strength and stiffness values determined from mechanics of materials considerations, and bearing and bearing seat dimensions. Limit states for abutments were based entirely on displacement of the abutment and limiting displacement values given in HAZUS99 [25]. Separately, the likelihood of soil liquefaction was investigated for each earthquake using the procedure outlined by Kayen and Mitchell [26]. To facilitate the construction of component fragility curves, these limit states were correlated with the damage states of HAZUS99 [25], as listed in Table 1.

To construct component fragility curves for step 6, $\ln(S_d)$ versus $\ln(PGA)$ plots, similar to the one shown in Figure 6, were constructed for each component in each model-earthquake pair (S_d is the seismic demand on the component). Regression analysis was then used to determine the unknown coefficients in the following equation:

$$\ln(S_d) = a \ln(PGA) + b$$

Once the seismic demand was known, the component fragility curves were determined using the following equation:

$$P_f = \Phi \left[\frac{\ln(S_d/S_c)}{\sqrt{\beta_d^2 + \beta_c^2}} \right]$$

where $\Phi[. . .]$ is the standard normal distribution function, S_c is the seismic capacity, and the denominator of the argument is the dispersion constant taken from HAZUS99 [25]. This assumes that the component capacity and seismic demand can be described by a lognormal distribution.

Once fragility curves for each component had been determined, first order reliability theory was used to provide upper and lower bounds to the system fragility curve. The lower bound curve was simply given by

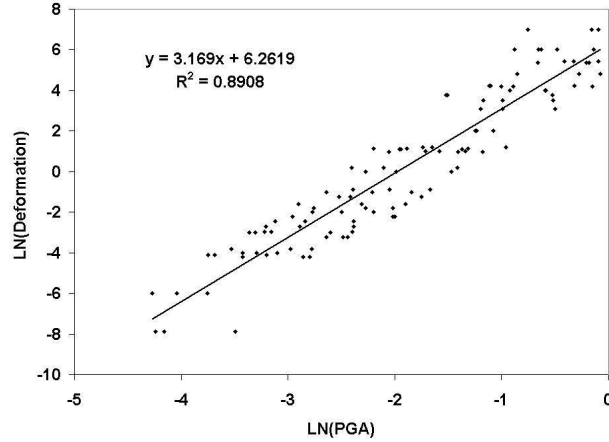


Figure 6 Component $\ln(S_d)$ versus $\ln(PGA)$ Plot

the maximum component fragility, while the upper bound curve was constructed from an aggregation of all of the component fragilities. The following expression summarizes this:

$$\max_{i=1}^m [P(F_i)] \leq P(F_{sys}) \leq 1 - \prod_{i=1}^m [1 - P(F_i)]$$

where $P(F_i)$ is the probability of the i^{th} component reaching or exceeding the given damage state and $P(F_{sys})$ is the probability that the system will reach or exceed the given damage state. The upper bound curves were taken as the system fragility curves, thus completing step 7.

IDOT BRIDGE 067-0021 FRAGILITY CURVES

Component Fragility Curves

Figure 7 shows the four most critical component damage state curves of IDOT bridge 067-0021 for the extensive and complete damage categories. In both damage state categories, foundation component limit states control. In the extensive damage category, shear in the pile cap at the wall face controls for PGA values below approximately 0.65g (where g is the acceleration due to gravity), whereas for PGA values above approximately 0.65g, axial-moment loading in the piles controls. The limiting shear stress value

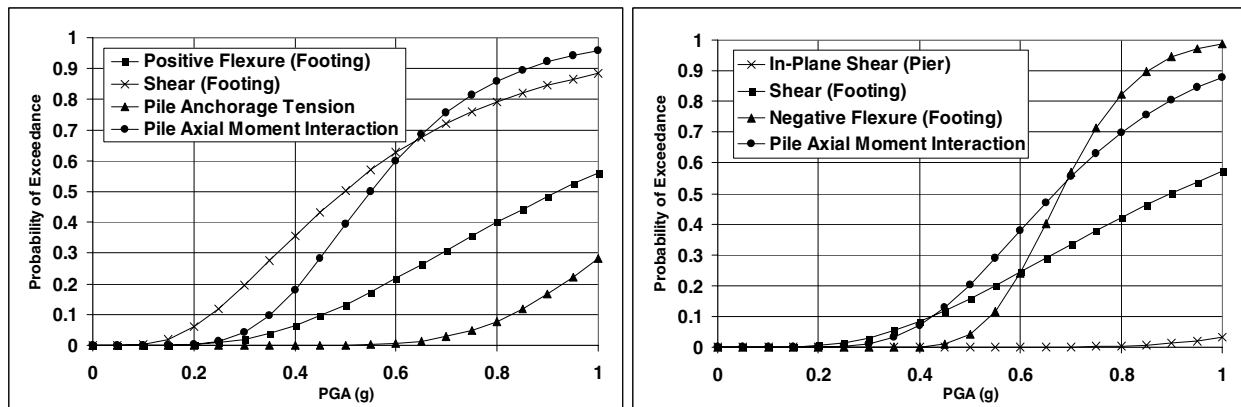


Figure 7 IDOT Bridge 067-0021 Component Damage Curves for the Extensive Damage Category (Left) and the Complete Damage Category (Right)

was set equal to the value obtained from ACI 318-02 [21], and the limiting axial-moment interaction value was taken as the value specified by Viest et al. [23].

In the complete damage category, shear in the pile cap at the wall face and axial-moment loading in the piles are the controlling component limit states for PGA values below 0.7g, whereas for PGA values greater than 0.7g, negative bending moment flexure in the pile cap at the wall face is the controlling component limit state. The limiting footing shear stress was taken as 1.5 times the value calculated from ACI 318-02 [21]. A value larger than the limiting value specified in ACI 318-02 was used based on the assumption that a localized shear stress in excess of the value specified by ACI 318-02 would not necessarily signify catastrophic shear failure throughout a significant portion of the pile cap. The limiting value for axial-moment interaction in the piles was taken as 1.25 times the value specified by Viest et al. [23]. Similarly, this value exceeds the true capacity of an individual pile, but it was felt that complete damage would only occur in the event of several piles failing due to axial-moment loading. The pile cap contained only bottom reinforcement and had no top reinforcement for resisting a negative bending moment once the concrete tensile capacity had been exceeded; therefore the limiting negative flexure capacity was calculated assuming that flexural cracking at the top surface of the footing led to total failure.

Each of the controlling limit states for the extensive and complete damage categories is realized in a brittle fashion, with the possible exception of axial-moment loading failures in the piles. The trend towards failure mechanisms that are brittle and that occur in the difficult to access and assess pile cap and pile foundation system is problematic. Brittle failures of this nature could cause a sudden loss in stiffness and/or strength within one of the major load carrying mechanism of the bridge, potentially leading to increased damage or injury. Determining whether these failures have occurred, or determining the particular state of damage that any one of these vulnerable foundation components has sustained, could be difficult or impossible.

Structure Fragility Curves

Figure 8 shows the upper bounds to the fragility curves for IDOT bridge 067-0021. It is clear from the plot that IDOT bridge 067-0021 is highly susceptible to all damage levels above a PGA of about 0.6g. Even at relatively modest PGA levels, the structure has a high probability of experiencing moderate damage and a non-negligible probability of experiencing extensive damage. In the East St. Louis area, for example, where this bridge is located, USGS lists expected PGA values of approximately 0.1g and 0.3g for 10% and 2% PE in 50 years events, respectively [27]. In those events, the structure could be expected to perform relatively well, with probabilities of 96%, 59%, 24%, and 4% of reaching or exceeding the slight/minor, moderate, extensive, and complete damage states, respectively. However, locations in extreme southern Illinois have PGA values listed at upwards of 1.7g for a 2% PE in 50 years event [27]. In such an event, the structure would most likely be expected to experience complete failure. Table 2 lists expected PGA values for three southern Illinois cities. From the table it can be concluded that bridges of this type, located as far north as Carbondale, would have a high probability of experiencing complete failure in a 2% PE in 50 years event.

City	10% PE in 50 Years	5% PE in 50 Years	2% PE in 50 Years
East St. Louis	0.09g	0.16g	0.28g
Carbondale	0.17g	0.31g	0.59g
Cairo	0.22g	0.63g	1.67g

Table 2 Expected PGA Values for Three Southern Illinois Cities According to USGS

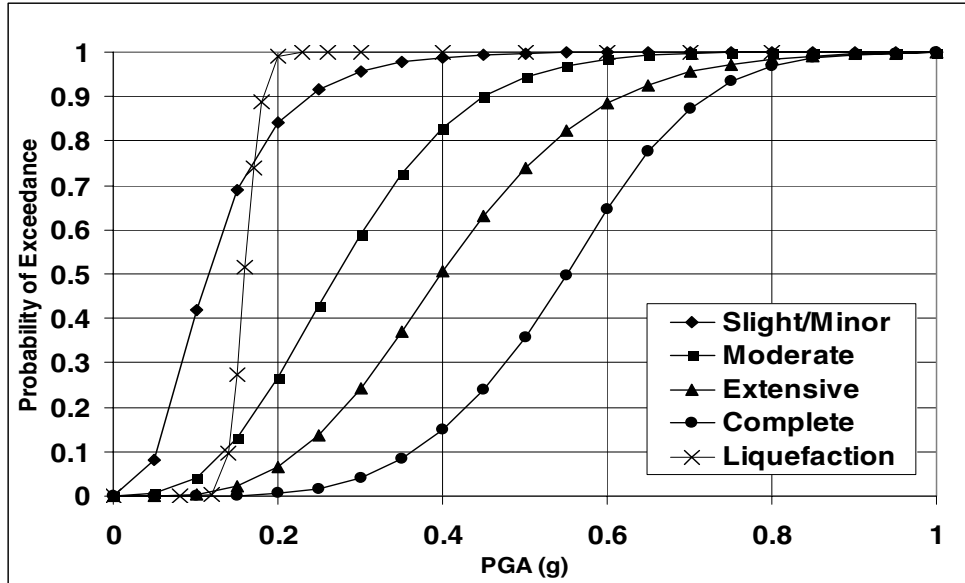


Figure 8 IDOT Bridge 067-0021 Fragility Curves

Overlain on Figure 8 is the liquefaction fragility curve for the bridge site. It is interesting to note that for any level of ground shaking with a PGA value above approximately 0.15g, the liquefaction fragility curve dominates the bridge fragility. Even for the relatively modest 2% PE in 50 years PGA value for East St. Louis, the bridge site would have an extremely high likelihood of experiencing liquefaction. Some care should be exercised here, since liquefaction susceptibility is highly dependent on local soil conditions, and such a high vulnerability to liquefaction may not be the norm for other bridge locations. With that being said, though, the local soil conditions at IDOT bridge 067-0021 do not vary drastically from soil conditions at many other wall pier bridge sites investigated in the wall pier bridge survey mentioned earlier. If this is indeed the case and in fact this trend occurs throughout southern Illinois, then soil liquefaction during a 10% PE in 50 years event could potentially inflict large levels of damage on southern Illinois bridges (and their adjoining at-grade highways), crippling large portions of the emergency transportation network.

SOUTHERN ILLINOIS PRIORITY EMERGENCY ROUTE VULNERABILITY

Of the estimated 595 bridges on southern Illinois priority emergency routes, approximately 86% of those bridges are either multi-column pier supported or wall pier supported. As reported by Zhong [4], approximately 61% of the multi-column pier supported bridges would be expected to experience major (or complete in this study) damage in a 2% PE in 50 years event. For a similar level of shaking, upwards of 100% of the wall pier bridges in extreme southern Illinois locations may be expected to experience complete damage, approximately 65% may be expected to experience complete damage in portions of southern Illinois as far north as Carbondale, and approximately 4% may be expected to experience complete damage as far north as East St. Louis. Based on these findings and the respective percentages of multi-column pier supported and wall pier supported bridges on southern Illinois priority emergency routes, the number of bridges experiencing complete damage could potentially reach half of the total number of bridges on the priority emergency routes. When the effects of liquefaction are considered, the number of wall pier bridges experiencing complete damage could likely increase, further boosting the total number of bridges experiencing complete damage in a 2% PE in 50 years event.

For a 10% PE in 50 years event, the transportation network would likely perform better. Zhong reported that in such an event multi-column pier supported bridges would likely only experience minor damage. The wall pier bridges would likely be less vulnerable to such levels of shaking as well. Essentially only wall pier supported bridges located in the extreme southern portions of the state of Illinois would be subjected to shaking strong enough to cause more than slight/minor damage. However, this assessment neglects any damage that could potentially be caused by liquefaction of soils at each bridge site. When the vulnerability to liquefaction is included, the performance of the emergency transportation network in a 10% PE in 50 years event is somewhat less certain.

CONCLUSIONS

Fragility analysis of a single wall pier supported bridge, typical of those found on southern Illinois priority emergency routes, has demonstrated the vulnerability of these types of structures to seismic events. The failure modes of shearing of the pile cap at the wall face and pile failure due to axial-moment loading were found to control for the extensive damage category; pile failure due to axial-moment loading and failure of the footing due to negative bending moment flexure was found to control for the complete damage category. If the effects of soil liquefaction are neglected, the bridge is expected to perform relatively well for 2% and 10% PE in 50 years events in the East St. Louis area, but poorly for similar events in regions of extreme southern Illinois. This information, in conjunction with the results from a multi-column pier supported bridge vulnerability study conducted by Zhong [4], provides an indication of the high vulnerability of southern Illinois priority emergency routes to seismic loading.

ACKNOWLEDGEMENTS

This work was funded in part by the Illinois Department of Transportation (IDOT) as part of IDOT Grant IHR-R36 ("Assessment of the Seismic Vulnerability of Wall Pier Supported Bridges on Emergency Priority Routes in Southern Illinois"). IDOT's financial support and the capable assistance of IDOT bridge engineer Tom Domagalski are greatly appreciated.

REFERENCES

1. Stover CW, and Coffman JL. "Seismicity of the United States, 1568-1989 (Revised)." U.S. Geological Survey Professional Paper 1527; Washington, DC: United States Government Printing Office, 1993.
2. Nuttli OW. "The Effects of Earthquakes in the Central United States." Third Edition. Marble Hill, MO: Guttenberg-Richter Publications, 1995.
3. Illinois Department of Transportation. "Earthquake Preparedness Plan 2001." Springfield, IL: Illinois Department of Transportation, Bureau of Operations, 2001.
4. Zhong Q. "Assessing the Effectiveness of Reducing Seismic Vulnerability by a Program of Bridge Pier Wrapping." PhD thesis, University of Illinois at Urbana-Champaign, 2001.
5. Bignell J, LaFave J, Hawkins N. "General Characteristics of Wall Pier Supported Bridges." Task I Interim Report. Springfield, IL: Illinois Department of Transportation, 2003.
6. Hibbit, Karlsson & Sorensen, Inc. "ABAQUS Standard User's Manual: Version 6.3." Pawtucket, RI, 2002.
7. Bignell J, LaFave J, Hawkins N. "Wall Pier Bridge Modeling Overview." Task II Interim Report. Springfield, IL: Illinois Department of Transportation, 2003.
8. Applied Technology Council. "Improved Seismic Design Criteria for California Bridges: Provisional Recommendations." ATC-32. Redwood City, CA, 1996.

9. Inel M. "Displacement-Based Strategies for the Performance-Based Seismic Design of "Short" Bridges Considering Embankment Flexibility." PhD thesis, University of Illinois at Urbana-Champaign, 2002.
10. Mander JB, Kim DK, Chen SS, Premus G. "Response of Steel Bridge Bearings to Reverse Cyclic Loading." Technical Report NCEER-96-0014. Buffalo, NY: State University of New York at Buffalo, 1996.
11. Wissawapaisal C. "Modeling the Seismic Response of Short Bridge Overcrossings." PhD thesis. University of Illinois at Urbana-Champaign, 2000.
12. Ash C, Schwartz J, Aschheim M, Hawkins N, Gamble B. "Evaluation of Elastomeric Bridge Bearings for Seismic Design." Report No. ITRC FR 99-4. Springfield, IL: Illinois Transportation Research Center, Illinois Department of Transportation, 2002.
13. Meymand P. "Shaking Table Scale Model Tests of Nonlinear Soil-Pile-Structure Interaction in Soft Clay." PhD thesis. University of California, Berkeley, 1998.
14. Wang S, Kutter B, Chacko J, Wilson D, Boulanger R, Abghari A. "Nonlinear Seismic Soil-Pile Structure Interaction." *Earthquake Spectra* 1998;12(2): 1425-1445.
15. Kornkasem W. "Seismic Behavior of Pile-Supported Bridges." PhD thesis. University of Illinois at Urbana-Champaign, 2001.
16. Choi E, DesRoches R, Nielson B. "Seismic Fragility of Typical Bridges in Moderate Seismic Zones." *Engineering Structures* 2004; 26(2): 187-199.
17. Wen YK, Wu CL. "Uniform Hazard Ground Motions for Mid-America Cities." Mid-America Earthquake Center: University of Illinois at Urbana-Champaign, 1999. (<http://mae.cee.uiuc.edu/newsite/ProjectWebs/RR-1/GMotions/Index.html>)
18. Ordonez GA. "SHAKE2000 Computer Program for the 1-D Analysis of Geotechnical Earthquake Engineering Problems: User's Manual." 2003. (<http://www.shake2000.com>)
19. Haroun MA, Pardoen GC, Shepard R, Haggag HA, Kazanjy RP. "Cyclic Behavior of Bridge Pier Walls for Retrofit." Final Report to the California Department of Transportation. Irvine, CA: University of California at Irvine, 1993.
20. Abo-Shadi NA, Saiidi M, Sanders DH. "Seismic Response of Bridge Pier Walls in the Weak Direction." Report to the Multidisciplinary Center for Earthquake Engineering Research (MCEER) Report No. CCEER-99-3. Reno, NV: University of Nevada, Reno, 1999.
21. American Concrete Institute. "Building Code Requirements for Structural Concrete and Commentary." ACI 318-02 and ACI 318R-02. Farmington Hills, MI; 2002.
22. Alsiwat JM, Saatcioglu M. "Reinforcement Anchorage Slip Under Monotonic Loading." *Journal of Structural Engineering* 1992; 118(9): 2421-2438.
23. Viest IM, Colaco JP, Furlong RW, Lawrence GG, Leon RT, Wyllie LA. "Composite Construction Design for Buildings." New York, NY: McGraw-Hill, 1997.
24. American Institute of Steel Construction, Inc. "Manual of Steel Construction, Load and Resistance Factor Design." Third Edition. Chicago, IL; 2001.
25. Federal Emergency Management Agency. "Earthquake Loss Estimation Methodology: HAZUS99 Technical Manual." Washington, DC: 1999. (<http://www.fema.gov/>)
26. Kayen R, Mitchell J. "Assessment of the Liquefaction Potential During Earthquakes by Arias Intensity." *Journal of Geotechnical and Geoenvironmental Engineering* 1997; 123(12): 1162-1174.
27. Frankel A, Mueller C, Barnhard T, Perkins D, Leyendecker E, Dickman N, Hanson S, Hopper M. "National Seismic Hazard Maps: Documentation." Open-File Report 96-532. Department of the Interior: U.S. Geological Survey, 1996.